

Novel Miniature Reconfigurable Microwave Filters

B. Dunne⁽¹⁾, L. Kennedy⁽¹⁾, J. Hong⁽²⁾, T. Corless⁽¹⁾, D. Gotch⁽³⁾ and M. Haynes⁽⁴⁾

⁽¹⁾ INEX, Newcastle University, Herschel Building, Newcastle NE1 7RU

⁽²⁾ Heriot-Watt University, Edinburgh EH14 4AS

⁽³⁾ Filtronic Defence Limited, Acorn Park, Shipley, Yorkshire, BD17 7SW

⁽⁴⁾ Selex Sensors & Airborne Systems Ltd., Capability Green, Luton, Bedfordshire, LU1 3PG

Abstract

Based on standard semiconductor fabrication techniques, a tunable, reconfigurable notched RF filter has been designed which utilises a MEMS micro-bridge structure as the switching component. Using this design, both RF filter and switch have been fabricated independently of one another to allow unhindered assessment of each component thereby minimising risks associated with fabrication of a fully integrated device. RF test results of fabricated filters show encouraging correlation with theory in the 1 – 8GHz range, and actuation of a MEMS contact switch has been demonstrated using an actuation voltage of 120V. Initial findings from this year's activities will feed into subsequent design iterations.

Introduction

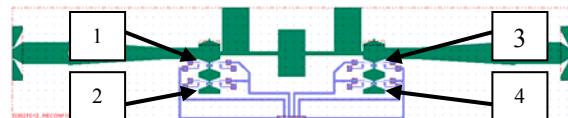
Reconfigurable multifunction filters are of increasing importance in RF and microwave systems, in part driven by fragmentation of military RF frequency bands through sale by governments of RF sub-bands for civilian applications. For most current systems, the physical volume of the RF front-end is dominated by the size of the necessary filters. The trend for most RF systems applications is therefore towards smaller, lighter systems with increased functionality including multi-function, multi-application equipment.

This paper describes the design and prototype fabrication of both a notched RF filter and a MEMS contact switch, with the intention of integrating the two to provide a reconfigurable RF filter.

Notched Filter Design

The type of filter to be investigated in this work is that of a “notched” filter. The “notch” refers to an artefact of the resultant frequency response curve where a portion of the spectrum is attenuated at a specific

frequency through a change in the physical structure of the filter. A reconfigurable filter can therefore be created through use of switches to introduce or remove appropriate geometrical elements from the filter. A prototype design incorporating four switches is shown in fig. 1. The modelled frequency response of this design is reproduced in fig. 2. Configuration 1 (C1) represents the filter characteristic for all 4 switches in the off-state. Configuration 2 (C2) is the filter characteristic with all 4 switches in the on-state. Configuration 3 (C3) shows how the notch frequency can be moved by placing switches 1 and 3 in the on-state and switches 2 and 4 in the off-state.



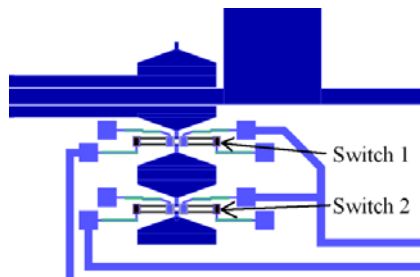


Fig. 1. Prototype four switch “notched” filter layout (top) and close-up of two of the four switches (bottom).

Filter Fabrication

Filters were fabricated on 6” quartz substrates with blanket layers of Ti/Au on both sides of the wafer. One side was patterned with the modelled filter design as described in the preceding section and electroplated to the required thickness to take into account the effects of skin depth. The wafer was then diced with each die electroplated on the underside of the wafer to form a ground plane. These devices were then tape-bonded to connect the ground plane to the filter layer. To decouple the performance of the filter from the performance and possible fabrication difficulties associated with the switch, initial prototypes replaced the three possible switch configurations described above with corresponding permanent metal contacts.

RF Test Results

RF test results for the configurations corresponding to C1, C2, and C3 are shown in fig. 3. These correlate well with the simulation (fig. 2) in the 1 – 8 GHz range, but exhibit insertion loss roll-off toward higher frequencies.

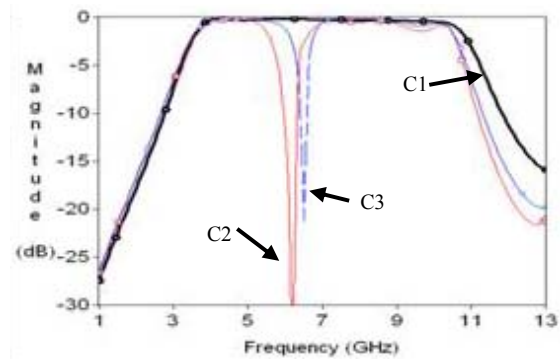


Fig. 2. Modelled frequency characteristics of the “notched” RF filter showing the three possible configurations the switches will take. C1 represents the filter characteristic for all 4 switches in the off-state. C2 is the filter characteristic with all 4 switches in the on-state. Configuration 3 (C3) shows how the notch frequency can be moved by placing switches 1 and 3 in the on-state and switches 2 and 4 in the off-state.

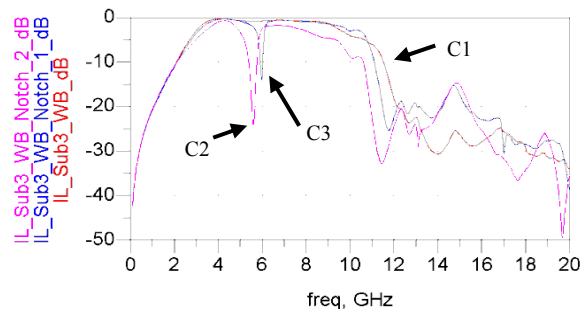


Fig. 3. RF test results for prototype filters.

MEMS Switch Design

There are two main failure modes to note when discussing MEMS switches [1]. The first applies predominately to capacitive switches where charge trapping in the dielectric layer between actuating electrodes as well as between capacitive contact areas can cause stiction of the bridge in the closed position. Stiction can be characterised as an undesired force which holds the switch in the closed position, long after any actuation voltage has been removed and may render the switch un-useable for most applications.

The second failure mode applies mainly to contact switches and more specifically the contact areas themselves. Contact degradation can limit the useful lifespan of

the switch as well as changing the contact resistance of the metal contacts themselves.

These potential failures were considered

Frequency	1GHz	5GHz	10GHz	18GHz
Insertion Loss	0.1dB	0.2dB	0.3dB	0.5dB
Return Loss	>20dB	>18dB	>15dB	>10dB
Isolation	>50dB	>35dB	>30dB	>25dB

when designing the MEMS switch and consequently, platinum has been used for the switch contacts to try and improve the life-span of the device.

The switch design used was that of a silicon nitride bridge structure with each end of the bridge permanently anchored to the substrate. Two electrostatic actuation pads are located underneath the bridge, one on either side of the filter transmission line (T-line) contact area (fig. 4). Voltage applied to these pads provides the mechanism to pull the switch down into the closed state through bending of the bridge. The switch opens upon removal of the actuation

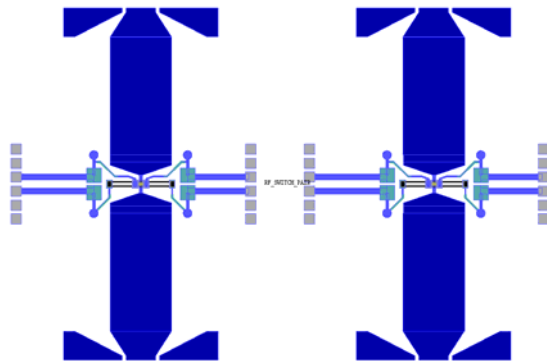


Fig. 4. Layout of two test switches as fabricated. The thick vertical lines are the T-lines. The switch micro-bridges are shown horizontally in the middle of each T-line.

voltage through the restoring force

Frequency	1GHz	5GHz	10GHz	18GHz
Insertion Loss	0.1dB	0.2dB	0.4dB	0.6dB
Return Loss	>15dB	>13dB	>10dB	>8dB
Isolation	>35dB	>27dB	>22dB	>18dB

associated with the inherent stress in the bent bridge structure.

Modelling of the electrical parameters of this design has been carried out as a function of substrate thickness, and the results are summarised in Tables 1 and 2.

Table 1. Selected frequency characteristics for a modelled MEMS switch on a 500 μm quartz substrate.

Table 2. Selected frequency characteristics for a modelled MEMS switch on a 50 μm quartz substrate.

MEMS Switch Fabrication

The switch was fabricated on a 6" quartz substrate with a dielectric constant of 4.1 at 1MHz and loss factor 0.0002 at 1 MHz [2]. A lift-off photo-resist process was used to pattern the T-line and DC actuation control lines with NiCr/Au deposited via sputtering. This layer was then patterned to allow removal of the top Au layer via wet etching to form the resistive elements in the DC actuation lines. A PECVD SiN layer was deposited with apertures to allow access to the anchor points, probe pads and T-line contact regions being plasma etched. Another lift-off process was then used with evaporated Ti/Pt to form the contact metallisation for the T-line (fig. 5a).

The next step in the processing sequence was sacrificial layer deposition (fig. 5b). The sacrificial layer was then patterned and plasma etched to form the anchor regions and probe pad openings.

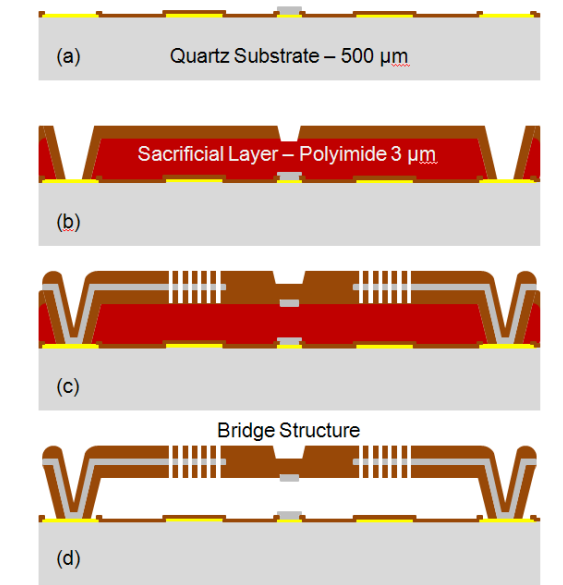


Fig. 5. Process flow for the MEMS switch: (a) The transmission line (T-line), actuation lines and probe pads are fabricated. (b) Sacrificial layer and lower bridge layer are deposited and patterned. (c) Completion of the bridge structure. (d) Release process using an oxygen plasma.

The final part of fabrication concerns the bridge structure itself. Here, a silicon nitride layer was deposited by PECVD, then patterned and plasma etched to open up contact areas for the anchor bases as well as the contact region in the bridge. Ti/Pt/Au was evaporated on a lift-off resist pattern to form the actuation electrodes within the bridge as well as the metal contact in the bridge. A silicon nitride top layer was added and patterned to complete the bridge structure ready for release (fig. 5c). Prior to release, the T-line areas have the sacrificial layer and SiN etched, a TiAu seed layer deposited via sputtering, and are then electroplated to increase their thickness to accommodate the skin depth of the conductor up to an operating frequency of 20GHz.

An early prototype switch (fabricated on a silicon substrate) is shown in fig. 6. Later prototype switches were fabricated on quartz substrates.

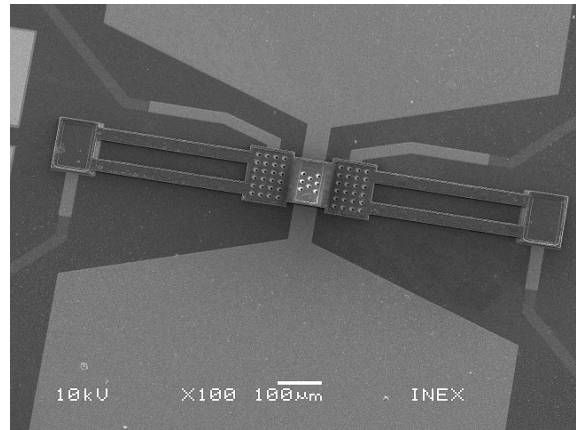


Fig. 6. SEM image of an early prototype MEMS switch fabricated on a 6" silicon substrate.

MEMS Switch Characterisation

Devices fabricated on quartz yielded switches that were successfully actuated at 120V. Design iterations to reduce the actuation voltage and potential stiction issues are in progress.

Conclusion

Test results for fabricated filter devices correlate well with theoretical modelling in the 1-8 GHz range, with increasing insertion loss roll-off observed at higher frequencies. This provides evidence that a practical reconfigurable filter can be fabricated through integration of the filter with appropriate MEMS switches.

Initial designs for the MEMS switch have been modelled for their RF performance and exhibit reasonable attributes; attributes that are improved by the use of thinner substrates. Prototype devices have demonstrated actuation under an applied 120V DC bias.

References

1. REBEIZ, G.M. and GUAN-LENG, T; *MEMS Switch Reliability and Power Handling*, Rebeiz, G (Ed.), RF MEMS Theory, Design and Technology (Wiley, NY, 2003), pp. 185-197
2. LIDE, D.R., *Dielectric Constants of Glasses*, Lide, D.R. (Ed.) Handbook of Chemistry and Physics (CRC Press, FL, 2003), p 12-63

Acknowledgements

The work reported in this paper was funded by the Electro-magnetic Remote Sensing (EMRS) Defence Technology Centre, established by the UK Ministry of Defence and run by a consortium of SELEX Galileo, Thales UK and Roke Manor Research.